THE JOURNAL OF PHYSICAL CHEMISTRY Letters

Cite This: J. Phys. Chem. Lett. 2018, 9, 2338−2345

Letter

pubs.acs.org/JPCL

Doubly Screened Hybrid Functional: An Accurate First-Principles Approach for Both Narrow- and Wide-Gap Semiconductors

Zhi-Hao Cui, Yue-Chao Wang, Min-Ye Zhang, Xi Xu, and Hong Jiang*

Beijing National Laboratory for Molecular Sciences, State Key Laboratory of Rare Earth Material Chemistry and Application, Institute of Theoretical and Computational Chemistry, College of Chemistry and Molecular Engineering, Peking University, 100871 Beijing, China

ABSTRACT: First-principles prediction of electronic band structures of materials is crucial for rational material design, especially in solar-energy-related materials science. Hybrid functionals that mix the Hartree−Fock exact exchange with local or semilocal density functional approximations have proven to be accurate and efficient alternatives to more sophisticated Green's function-based many-body perturbation theory. The optimal fraction of the exact exchange, previously often treated as an empirical parameter, is closely related to the screening strength of the system under study. From a physical point of view, the screening has two extreme forms: the dielectric screening $[1/\epsilon_M]$ that is dominant in wide-gap materials and the Thomas−Fermi metallic screening $[\exp(-\zeta r)\ ]$ that is important in narrow-gap semiconductors. In this work, we have systematically investigated the performances of a nonempirical doubly screened hybrid (DSH) functional that considers both screening mechanisms and found that it excels all other existing hybrid functionals and describes the band gaps of narrow-, medium-, and wide-gap insulating systems with comparably good performances.

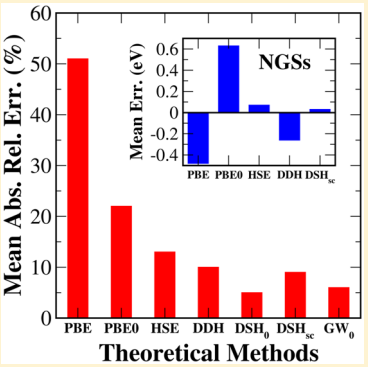

In recent years, first-principles electronic structure theory, represented by density functional theory (DFT) in the local density approximation (LDA) or various generalized gradient approximations (GGAs), has gained tremendous popularity in condensed matter physics and materials science.[1−3] However, the widely used local/semilocal approximate functionals have long been plagued by the systematic underestimation of the band gap of insulating materials,[4,5] especially for narrow-gap semiconductors (NGS), which are often wrongly described as metallic. Furthermore, closely related to this so-called "band gap problem", the first-principles description of a lot of other properties, such as the defect formation energy[6] and the ionization potential of semiconducting materials,[7−12] also exhibits significant errors. In contrast, hybrid functionals that mix a fraction of Hartree−Fock (HF) exact exchange with LDA/GGAs can provide significant improvement for those properties as well as the band gap. Commonly used hybrid functionals such as PBE0,[13,14] which incorporates 1/4 of the Hartree−Fock exact exchange, HSE,[15,16] which is similar to PBE0 but uses a screened Coulomb interaction for the exact exchange part with an empirically determined screening parameter, and the well-known B3LYP functional,[17,18] have been widely tested in description of the band gap and thermodynamic properties of semiconductors.[19−23] Despite their significantly improved performances in describing the electronic band structure of typical semiconductors with respect to LDA/GGA,[23] the accuracy of each hybrid functional tends to be limited to a certain class of materials. For example, the HSE functional with the empirically determined screening parameter performs very well in describing semiconductors with the band gap falling in the range of 1−3 eV but tends to underestimate the band gaps of wide-gap insulators. Similar problems also exist for other hybrid functionals with fixed parameters.[24−26]

Many-body perturbation theory in the *GW* approximation[27,28] has been systematically developed in the past decades and is regarded as one of the most accurate approaches to electronic band structure properties of materials.[4,29−31] Unlike many other methods, the *GW* method is able to describe the band gaps of various normal insulating materials with essentially comparable accuracy. One of the most important features of the *GW* method is its capability to accurately describe screening effects of different strength in different materials. The success of the hybrid functionals can also be rationalized based on the *GW* description of screening effects.[26,32,33] In particular, it has been noted that the fraction of the Hartree−Fock exact exchange α_{HF} is closely related to the screening strength of the system, as described by its macroscopic dielectric constant (ϵ_M), which is system-dependent. On the basis of such a link between α_{HF} and ϵ_M, several new hybrid functional approaches have been proposed recently.[26,32−36] In this work, we further exploit the link between the *GW* approach and the hybrid functionals and emphasize the importance of considering both dielectric screening (dominant in insulators) and short-range metallic screening (important for NGSs) in the hybrid functional framework for accurate description of both NGSs and wide-gap semiconductors.

As has been realized by many researchers,[26,32,37] the success of the hybrid functional approach to the band gap problem can

Received: March 26, 2018
Accepted: April 19, 2018
Published: April 19, 2018

DOI: 10.1021/acs.jpclett.8b00919
J. Phys. Chem. Lett. 2018, 9, 2338−2345

be attributed to its relation to the *GW* approach. In particular, it can be regarded as a further approximation to the Coulomb hole and screened exchange (COHSEX) approximation to the *GW* exchange−correlation self-energy, which can be obtained by neglecting the frequency dependence of the screened Coulomb interaction W in the *GW* self-energy[28]

$$\begin{aligned}\Sigma_{xc}(\mathbf{r}, \mathbf{r}') &= -\frac{1}{2}\delta(\mathbf{r}-\mathbf{r}')[\nu(\mathbf{r}, \mathbf{r}') - W(\mathbf{r}, \mathbf{r}'; \omega = 0)] \\ &\quad - \sum_{i=1}^{N_{occ}} \psi_i(\mathbf{r})\psi_i^*(\mathbf{r}')W(\mathbf{r}, \mathbf{r}'; \omega = 0) \\ &\equiv \Sigma_{COH}(\mathbf{r}, \mathbf{r}') + \Sigma_{SEX}(\mathbf{r}, \mathbf{r}') \end{aligned} \tag{1}$$

The screened Coulomb potential W above is defined as

$$W(\mathbf{r}, \mathbf{r}'; \omega) = \int d\mathbf{r}''\, \epsilon^{-1}(\mathbf{r}, \mathbf{r}''; \omega)\nu(\mathbf{r}'', \mathbf{r}') \tag{2}$$

where $\epsilon^{-1}(\mathbf{r},\mathbf{r}'';\omega)$ is the inverse dielectric function and $\nu(\mathbf{r}'',\mathbf{r}')$ denotes the bare Coulomb potential. In the following formalism, we use $\nu_{sc}(\mathbf{r},\mathbf{r}')$ to denote the static approximation to W, i.e., $\nu_{sc}(\mathbf{r},\mathbf{r}') \equiv W(\mathbf{r},\mathbf{r}';\omega{=}0)$. The main effect of the inverse dielectric function is to reduce the effective strength of electron−electron interaction, and the simplest approximation is to replace $\epsilon^{-1}(\mathbf{r},\mathbf{r}'')$ by a constant scaling factor equal to the inverse of the macroscopic dielectric constant $1/\epsilon_M$, such that

$$\Sigma_{SEX}(\mathbf{r}, \mathbf{r}') \approx -\frac{1}{\epsilon_M}\gamma(\mathbf{r}, \mathbf{r}')\nu(\mathbf{r}, \mathbf{r}') \tag{3}$$

where we introduce the first-order reduced density matrix

$$\gamma(\mathbf{r}, \mathbf{r}') \equiv \sum_{i=1}^{N_{occ}} \psi_i(\mathbf{r})\psi_i^*(\mathbf{r}') \tag{4}$$

When approximating the local COH term by LDA or GGA, this gives the dielectric-dependent hybrid (DDH) functional.[26,32] Marques et al.[32] proposed using $1/\epsilon_M$ calculated at the LDA/GGA level as the system-dependent α_{HF} and obtained quite good agreement with experiment for many semiconductors. Skone et al.[26] found that a self-consistent determination of α_{HF} can further improve the agreement with experiment for theoretical prediction of band gaps of typical sp insulating materials.[26] The self-consistent DDH functional has been used for a variety of different systems[33,38−41] and also extended to finite systems.[42]

From a physical point of view, the DDH approach only grasps one aspect of screenings in real solids, i.e., that of the dielectric screening, which is dominant in wide-gap insulators. It is therefore not surprising that the most significant improvement of the DDH approach compared to PBE0 is observed in systems with large band gaps. For the latter, the PBE0 approach, with a fixed $\alpha_{HF} = 0.25$, often underestimates the band gap.[26,32] In contrast, the DDH approach uses significantly larger α_{HF} for those systems due to their smaller dielectric constants and therefore predicts significantly larger band gaps that are in better agreement with experiment.[35] On the other hand, the DDH approach still exhibits significant errors for systems with narrow band gaps.[33,35] Physically, it can be attributed to the fact that other screening mechanisms can become important for NGSs. In the limit of metallic systems, the Thomas−Fermi screening, in which the effective screened Coulomb interaction takes the form of the Yukawa potential, becomes dominant.[43] To describe the band gaps of materials of different nature in the hybrid functional framework, it is crucial to consider both dielectric and metallic screenings with system-dependent screening parameters. For that purpose, we take a similar strategy as that in ref 34 and use a simple model dielectric function[44]

$$\epsilon(q) = 1 + \left[(\epsilon_M - 1)^{-1} + \alpha\left(\frac{q}{q_{TF}}\right)^2\right]^{-1} \tag{5}$$

where q_{TF} denotes the Thomas−-Fermi screening parameter and $\alpha = 1.563$ is an empirical parameter introduced to better describe the dielectric function of typical semiconductors according to ref 44. The corresponding screened Coulomb potential takes the form of

$$\begin{aligned}\nu_{sc}(\mathbf{r}, \mathbf{r}') &= \int \frac{d\mathbf{q}}{(2\pi)^3}\frac{4\pi}{q^2}\frac{1}{\epsilon(q)}\exp(i\mathbf{q}\cdot(\mathbf{r}-\mathbf{r}')) \\ &= \frac{1}{\epsilon_M}\frac{1}{|\mathbf{r}-\mathbf{r}'|} + \left(1 - \frac{1}{\epsilon_M}\right)\frac{\exp(-\tilde{q}_{TF}|\mathbf{r}-\mathbf{r}'|)}{|\mathbf{r}-\mathbf{r}'|}\end{aligned} \tag{6}$$

where $\tilde{q}_{TF}$ is defined as an effective Thomas−Fermi screening parameter

$$\tilde{q}_{TF}^{\,2} \equiv \frac{q_{TF}^{\,2}}{\alpha}\left(\frac{1}{\epsilon_M - 1} + 1\right) \tag{7}$$

It is obvious that in eq 6 the first term corresponds to the dielectric screening, which considers the full range of a scaled Coulomb interaction, and the second term represents the metallic screening, which considers only the short-range contribution. To simplify the implementation, we further use the complementary error function (erfc) to approximate the second term in eq 6 following ref 34

$$\nu_{sc}(\mathbf{r}, \mathbf{r}') \approx \frac{1}{\epsilon_M}\frac{1}{|\mathbf{r}-\mathbf{r}'|} + \left(1 - \frac{1}{\epsilon_M}\right)\frac{\mathrm{erfc}(\mu|\mathbf{r}-\mathbf{r}'|)}{|\mathbf{r}-\mathbf{r}'|} \tag{8}$$

with $\mu = \frac{2\tilde{q}_{TF}}{3}$. Using the screened Coulomb interaction with both dielectric and metallic screening considered above, we obtain the following doubly screened hybrid (DSH) exchange−correlation potential

$$\begin{aligned}V_{xc}^{DSH}(\mathbf{r}, \mathbf{r}') &= \frac{1}{\epsilon_M}V_x^{HF}(\mathbf{r}, \mathbf{r}') + \left(1 - \frac{1}{\epsilon_M}\right)V_x^{HF,SR}(\mathbf{r}, \mathbf{r}'; \mu) \\ &\quad + \left(1 - \frac{1}{\epsilon_M}\right)V_x^{PBE,LR}(\mathbf{r}; \mu) + V_c^{PBE}(\mathbf{r})\end{aligned} \tag{9}$$

where

$$V_x^{HF,SR}(\mathbf{r}, \mathbf{r}'; \mu) = -\gamma(\mathbf{r}, \mathbf{r}')\frac{\mathrm{erfc}(\mu|\mathbf{r}-\mathbf{r}'|)}{|\mathbf{r}-\mathbf{r}'|} \tag{10}$$

and $V_x^{PBE,LR}(\mathbf{r})$ is the long-range part of the PBE exchange functional (the same one as that used in the HSE functional[15]), which is introduced to compensate the missing long-range contribution corresponding to the second term. The corresponding exchange−correlation energy can then be written as

$$E_{xc} = E_x^{HF}[\gamma(\mathbf{r}, \mathbf{r}'); \nu_{sc}] - E_x^{PBE}[\rho(\mathbf{r}); \nu_{sc}] + E_{xc}^{PBE}[\rho(\mathbf{r})] \tag{11}$$

DOI: 10.1021/acs.jpclett.8b00919
J. Phys. Chem. Lett. 2018, 9, 2338−2345

where the first and second terms are the Hartree−Fock and PBE exchange energies calculated using the screened Coulomb interaction ν_{sc}, respectively. We note that the consideration of the third term ($V^{PBE,LR}$), which is neglected in previous works,[34,45,46] is important to obtain a consistent description of both the potential and the total energy in the generalized Kohn−Sham framework.[47,48]

In practice, the work flow of DSH is illustrated in Figure 1. We have implemented the DSH approach in Vienna ab initio

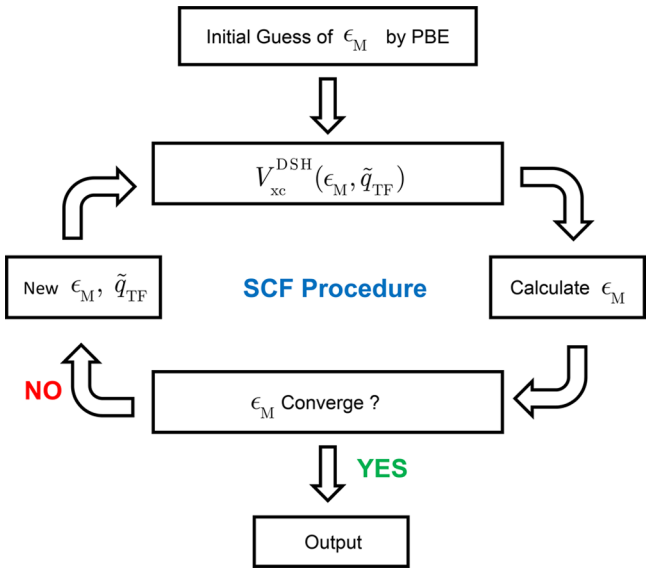

Figure 1. Illustration of the self-consistent procedure of the DSH functional.

simulation package (VASP),[49] based on its existing implementation of the screened hybrid functional module.[21] Several different approaches have been used for the calculation of the dielectric constant, including the Berry phase approach,[50−53] density functional perturbation theory (DFPT),[54,55] and the random phase approximation (RPA) method,[56] depending on the nature of the systems concerned. The Berry phase approach is the first choice because it is suitable for semiconductors and requires a relatively small **k**-mesh. For some systems, however, the band gap from PBE, which is used as the first step, is rather small, and thus, the Berry phase approach is no longer suitable due to the possible Zener tunelling.[57] Therefore, we use the DFPT method in the first step instead. The RPA approach is seldom used as it requires a summation of unoccupied states, usually on a fine **k**-mesh, and more importantly, it does not consider the local field effect.[24] The only cases for which we use the RPA approach are those with small band gaps. Besides the self-consistent DSH, we also consider the one-shot scheme that uses the dielectric constant from the PBE calculation without further updating, which is denoted as DSH_0 henceforth.

All calculations are performed by using the VASP code with the projector augmented-wave (PAW) approach to core−valence interactions.[58,59] Various density functional approximations have been used, including PBE GGA[60] and a series of hybrid functions, PBE0,[13] HSE06,[15,16] self-consistent DDH,[26] and our newly proposed DSH functional. The experimental crystal structures, with lattice constants taken from ref 61, are used to facilitate the comparison with experiment. The energy convergence criterion is chosen to be 10^{-6} eV for self-consistent field (SCF) iterations. By default, we use the ENMAX value in the PAW pseudopotential provided by VASP as the energy cutoff for the plane-wave expansion, unless otherwise specified, and a Γ-centered **k**-mesh of $N_k = 6 \times 6 \times 6$ is used for all cubic crystals. For noncubic crystals (such as those with the wurtzite structure), we take the number of **k** points along the axis of the smallest lattice constant to be 6, and those of the remaining axes are scaled to ensure roughly the same **k**-space spacing. We checked the convergence of the DSH calculation with respect to N_k in several representative semiconductors including Si, PbS, and ZnOw (ZnO in the wurtzite structure) by using a finer **k**-mesh of $8 \times 8 \times 8$ ($8 \times 8 \times 6$ for ZnOw) and found that the DSH band gaps change by less than 0.02 eV, indicating that our calculations are well converged with respect to N_k. The macroscopic dielectric constant used in the DDH and DSH approaches is taken as the maximal value of the diagonal elements of the dielectric constant tensor. The Thomas−Fermi screening parameter in the DSH approach is calculated in terms of the averaged valence electron density (including semicore d electrons for post-transition metal elements like Zn).

sp Semiconductors. We first investigate the performance of the DSH approach in both the one-shot and self-consistent schemes and make a comparison with other approaches for a set of typical sp semiconductors and insulators that are widely used as the test set for electronic band structure calculations of solids[19,23,62,63] due to their simplicity in both crystal and electronic structures and relatively well-compiled experimental measurements.[61,64] The band gaps calculated from different approaches are collected in Table 1.

Several features are noteworthy from Table 1. As expected, PBE significantly underestimates the band gaps of all considered systems by as much as 51% in terms of the mean absolute relative error (MARE). In particular, GaSb, a NGS, is predicted by PBE to be metallic once the correction from the spin−orbit coupling (SOC) is considered. For wide-gap semiconductors, the errors of PBE results can be several eV, which is certainly unacceptable for any realistic description of electronic band structure of real materials. By mixing 1/4 of the exact exchange with PBE exchange, PBE0 has improved the band gap description to a large extent, and the MARE is now reduced to be about 22%. A closer look at the PBE0 results clearly indicates that PBE0 tends to overestimate band gaps of NGSs and underestimate the band gaps of wide-gap insulators, which explains the fact the mean absolute error (MAE) of the PBE0 results is significantly larger than the mean error (ME). The difficulty of PBE0 can be overcome to some extent by the DDH approach, which can adjust the contribution of the exact exchange in terms of the screening strength. The MARE of the DDH results is reduced to 10%. The performances of the DDH approach indicated by our calculations are consistent with those of the previous study.[26] The screened hybrid functional HSE06, which differs from PBE0 by using a screened Coulomb interaction in the exact change part,[15,16] also shows significant improvement with respect to PBE0 with a MARE of 13%, especially for systems with a small or moderate band gap, but tends to underestimate the band gap of wide-gap insulators, even more strongly than PBE0.

We then turn to the results of the DSH approach that considers both dielectric and metallic screening with system-dependent screening parameters (see Figure 2 for a more clear illustration of the accuracy of DSH compared to experiment). Both the one-shot (DSH_0) and self-consistent (sc-DSH) schemes lead to theoretical prediction in good agreement

DOI: 10.1021/acs.jpclett.8b00919
J. Phys. Chem. Lett. 2018, 9, 2338−2345

Table 1. Band Gaps (in eV) of Typical sp Semiconductors Calculated by the One-Shot and Self-Consistent DSHs (Denoted as DSH_0 and sc-DSH, Respectively) Compared to Those from Other Approaches[a]

syste	ϵ_{PBE}	ϵ_{DSH}	PBE(SOC)	PBE0	HSE06	DDH	DSH_0	sc-DSH	GW_0	expt
C	5.76	5.62	4.11	6.09	5.32	5.51	5.63	5.66	5.87	5.48
Si	12.18	10.98	0.56	1.96	1.30	0.98	1.12	1.16	1.19	1.17
SiC	6.80	6.33	1.34	2.98	2.25	2.35	2.49	2.55	2.53	2.42
BN	4.57	4.36	4.41	6.52	5.75	6.33	6.52	6.60	6.61	6.4
BP	8.88	8.29	1.33	2.79	2.08	2.00	2.11	2.16	2.20	2.1, 2.4
AlNw	4.69	4.21	4.13	6.21	5.49	6.05	6.07	6.25	6.11	6.2−6.3
AlP	7.88	7.17	1.57	2.95	2.28	2.31	2.44	2.51	2.51	2.51
AlAs	8.99	7.96	1.33 (0.10)	2.66	2.00	1.95	2.15	2.22	2.17	2.1
AlSb	11.02	9.14	0.99 (0.22)	2.24	1.61	1.45	1.78	1.87	1.57	1.6
GaN	5.65	4.95	1.73	3.67	2.97	3.23	3.39	3.57	3.21	3.30
GaP	9.66	8.55	1.66	2.99	2.32	2.24	2.39	2.46	2.30	2.26
GaAs	12.43	10.09	0.48 (0.11)	1.95	1.33	0.99	1.42	1.51	1.23	1.42
GaSb	18.32	12.15	−0.06 (0.23)	1.30	0.70	0.27	0.72	0.86	0.51	0.81
InP	10.00	8.49	0.74	2.15	1.52	1.33	1.54	1.63	1.27	1.34
ZnO	5.10	3.39	0.65	3.03	2.34	3.30	3.23	4.02	3.32	3.4
ZnOw	5.07	3.38	0.78	3.18	2.49	3.46	3.40	4.19	3.55	3.4
ZnS	5.81	4.85	2.07	3.96	3.30	3.51	3.83	4.04	3.61	3.68
ZnSe	7.03	5.59	1.15 (0.13)	2.91	2.28	2.26	2.73	2.95	2.54	2.7
ZnTe	8.55	7.09	0.98 (0.27)	2.50	1.88	1.75	1.91	2.04	2.02	2.26
CdSw	6.11	4.91	1.19	2.86	2.18	2.45	2.60	2.84	2.38	2.49
CdSew	7.53	5.64	0.55 (0.12)	2.11	1.51	1.50	1.81	2.05	1.54	1.75
CdTe	8.37	6.88	0.48 (0.28)	1.87	1.27	1.21	1.27	1.40	1.34	1.43
MgS	5.30	4.81	2.78	4.50	3.78	4.17	4.24	4.36	4.48	4.5
MgO	3.12	2.66	4.73	7.20	6.46	8.37	8.20	8.70	8.01	7.83
LiF	2.02	1.77	9.23	12.29	11.55	16.11	15.71	16.45	15.13	14.20
NaCl	2.44	2.24	5.08	7.15	6.44	8.83	8.56	8.84	8.43	8.5
ME			−1.61	0.18	−0.51	−0.06	−0.07	0.29	0.01	
MAE			1.61	0.53	0.54	0.28	0.18	0.32	0.15	
MARE [%]			51	22	13	10	5	9	6	

[a]The first two columns show the dielectric constants calculated from PBE and sc-DSH. The following columns are band gaps from different methods. The last three rows show the mean error (ME), mean absolute error (MAE), and mean absolute relative error (MARE) of the results from different methods with respect to the experimental data.[61,64] For systems with heavy elements, the correction due to spin−orbit coupling has been taken into account by subtracting the SOC correction calculated by PBE (the value in parentheses). For comparison, we also show the results from PBE-based GW_0 with the numerically accurate LAPW+HLOs basis.[63]

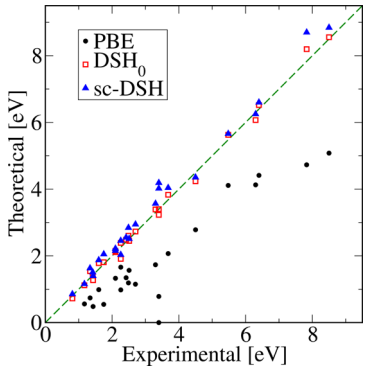

Figure 2. Calculated band gaps of sp semiconductors from PBE, DSH_0, and sc-DSH are plotted against corresponding experimental values.

with experiment, with the MARE smaller than 10%. For many systems, the DSH results agree well with those from numerically highly accurate GW_0@PBE calculations. The latter, taken from ref 63, are obtained by an all-electron implementation of *GW* with LAPW plus high-energy local orbitals (HLOs) basis. Generally speaking, the MARE within 10% is accurate enough for comparison with experiment due to the uncertainty of experimental preparations and measurements.[63] One can also see that the overall performance of the DSH_0 approach is even better than the sc-DSH approach for the selected set of semiconductors and insulators.

Narrow-Gap Semiconductors. NGSs are a class of important materials typically with a band gap of less than 0.5 eV, which are widely used in infrared detection and thermoelectrics.[65] Here we use NGS in a more broad sense and refer to semiconductors with experimental band gaps of less than 1 eV. The band gap of a NGS is much more difficult to predict accurately. LDA/GGA tends to predict it to be metallic, and in that case, even *GW*-based approaches can have difficulty because G_0W_0 or GW_0 with the qualitatively wrong LDA/GGA starting point cannot give reliable results, and other *GW* variants like hybrid functionals-based G_0W_0 or quasi-particle self-consistent *GW* (QSGW)[66] tend to significantly overestimate the band gap.[67]

Here we select a series of NGSs, namely, Ge, GeTe, SnSe, GaSb, InX (X = N, As, Sb), and PbX (X = S, Se, Te), and calculate their band gaps by PBE, PBE0, HSE06, DDH, and DSH functionals; see Table 2. The results clearly show that PBE completely fails for the selected set of NGSs and predicts most of them as metallic once the SOC effect is taken into account. On the other hand, PBE0 systematically overestimates the band gaps of these systems, with an overall MARE of

DOI: 10.1021/acs.jpclett.8b00919
J. Phys. Chem. Lett. 2018, 9, 2338−2345

Table 2. Band Gap of NGSs from Different Functionals[a]

system	PBE (SOC)	PBE0	HSE06	DDH	sc-DSH	expt
Ge	0.00 (0.06)	1.37	0.75	0.29	0.77	0.74
GeTe	0.41 (0.09)	1.22	0.66	0.47	0.48	0.61
SnSe	0.50 (0.03)	1.53	0.95	0.68	0.89	0.9
GaSb	−0.06 (0.23)	1.30	0.73	0.27	0.85	0.81
InN	0.00 (0.00)	1.41	0.77	0.73	0.84	0.7−0.9
InAs	−0.11 (0.11)	1.01	0.43	−0.11	0.55	0.417
InSb	−0.23 (0.23)	0.88	0.31	−0.22	0.47	0.235
PbS	−0.06 (0.38)	1.01	0.42	0.26	0.32	0.29
PbSe	−0.17 (0.42)	0.86	0.29	0.01	0.22	0.15
PbTe	−0.04 (0.74)	0.91	0.34	0.09	0.07	0.19
ME [eV]	−0.48	0.63	0.05	−0.26	0.03	
MAE [eV]	0.48	0.63	0.07	0.26	0.08	
MARE [%]	116	189	28	65	28	

[a]The last three rows show the mean error (ME), mean absolute error (MAE), and mean absolute relative error (MARE) of results from different methods with respect to the experimental data.[61,64,68] Particularly, the experimental band gap of InN is from refs 69−71, and GeTe is from refs 72 and 73. For systems with heavy elements, the result has taken the SOC into account by subtracting the correction by PBE calculation (the value in parentheses; some values are taken from ref 74 and 75). The dielectric constants of InN, InAs, and InSb are calculated by the RPA method without the local field effect.

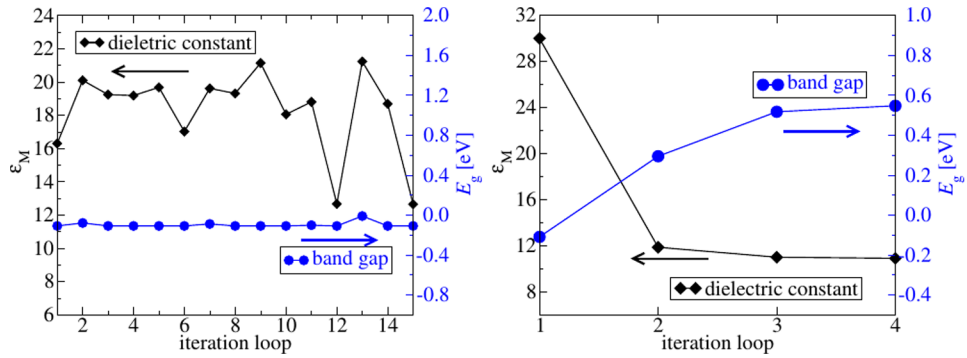

Figure 3. Calculated dielectric constant and band gap (with the SOC effect considered) of InAs plotted as a function of iteration steps by using the DDH (left) and DSH (right) approaches, respectively. A fine **k**-mesh of 16 × 16 × 16 is used in the DDH calculations, but a relatively small **k**-mesh of 6 × 6 × 6 is used for the DSH calculation.

+189%. The failure of PBE0 for NGSs can be attributed to its fixed hybrid coefficient of 1/4, considering that the dielectric constant of the narrow gap of a NGS is typically greater than 10. On the other hand, considering dielectric screening alone is not enough to obtain an accurate description of the band gap of a NGS, as clearly indicated by the results from the DDH approach. In the case of sp semiconductors, we have shown above that the DDH approach describes typical medium- and wide-gap semiconductors very well, consistent with the findings in ref 26. However, here for NGSs, DDH shows a systematic underestimation of band gaps, and the overall MARE is as large as 65%. In addition, we note that for some NGS systems the iteration in the DDH approach can have difficulty in reaching convergence. For example, the calculated dielectric constant in InAs jumps in a zigzag pattern, as shown in Figure 3 (left panel), and does not converge even after 15 iterations, in strong contrast to the situations in moderate- or wide-gap systems, where typically three or four iterations are enough to reach convergence. The convergence difficulty can be attributed to the fact that in a wide range of dielectric constants (about 12−24) the system is always metallic. Although the dielectric constants are different in iterations, the electronic band structures are, to a large extent, similar. We find that even if one takes the smallest dielectric constant (i.e., the maximum exact exchange ratio) among the iterations, it is still impossible to open a gap in InAs and InSb, which clearly indicates the drawback of the DDH approach for NGS systems. Furthermore, it is noteworthy that a metallic system often requires a finer **k**-mesh and a larger smearing value to get a convergent dielectric tensor. We test a series of **k**-mesh and find that for DDH, which describes InAs and InSb as metallic, more than 16 × 16 × 16 **k** points are needed, which inevitably leads to a great increase in computational cost. To make a rough estimation, the computational load is about 20 times larger, compared with a typical **k**-mesh of 6 × 6 × 6.

In contrast to DDH, the DSH approach is still effective for NGS systems, with a MAE of 0.08 eV and a MARE of 28%, which is already very close to the error bars of typical experimentally measured band gaps. Furthermore, DSH does not suffer from the convergence difficulty as DDH (the convergence can be readily reached after four iterations for InAs, as shown in Figure 3 (right panel)). The different performances of the DDH and DSH approaches clearly indicate that for NGS systems it is crucial to take into account both the dielectric screening and metallic screening.

Table 2 also shows the results from HSE06. We can see that HSE06 works as well as DSH for the selected NGS systems. Physically, the HSE functional also takes the form in which both dielectric and metallic screening are taken into account, but they are considered with fixed screening parameters: the

DOI: 10.1021/acs.jpclett.8b00919
J. Phys. Chem. Lett. 2018, 9, 2338−2345

dielectric screening is considered by using the same fraction of the exact exchange as PBE0 (i.e., $\alpha_{HF} = 0.25$), and the metallic screening is considered by using a range-separation parameter $\mu = 0.2$ Å^{-1} that is determined by empirical fitting of thermochemical data.[15] On the basis of the preceding discussion, we can see that the value of $\alpha_{HF} = 0.25$ is far from physical based on the calculated dielectric constants, but apparently due to a right combination of the values of α_{HF} and μ, the band gaps of many NGSs and moderate-gap semiconductors can be accurately predicted. The success of HSE06 compared to the failure of PBE0 clearly indicates the importance of considering the metallic screening for accurate description of band structure of NGSs. On the other hand, with system-independent screening parameters, we can not expect the HSE06 to be universally accurate for systems of different nature, as clearly indicated by the significant errors of HSE06 for the description of the band gaps of wide-gap semiconductors and insulators shown in Table 1.

To summarize, we have systematically explored the performances of a new range-separated hybrid functional, which takes both dielectric and metallic screenings into account with system-dependent and nonempirically determined screening parameters, for theoretical prediction of the band gaps of semiconductors and insulators with a wide range of band gap values. We found that all insulating systems with wide, moderate, or narrow band gaps can be well described by this DSH functional. In particular, for sp systems with moderate or wide band gaps, we find that both the one-shot (with PBE as the starting point) and self-consistent DSH can reproduce experimental results very well with a mean absolute relative error less than 10%, an accuracy that is comparable to numerically converged all-electron GW_0@PBE.[63] We have also investigated the performances of the self-consistent DDH approach[26] and found that DDH and DSH perform similarly in describing the electronic band structure of typical sp semiconductors with moderate and wide gaps. For NGSs, the DDH approach tends to significantly underestimate the band gaps and in some cases has difficulty in reaching convergence during iterative determination of dielectric constants. PBE0, which has a fixed fraction of the HF exact exchange, leads to severely overestimated band gaps. In contrast, the DSH still works very well, not only in terms of good convergence behavior but also in terms of quantitatively good agreement with experimental results. The overall remarkable performances of the DSH approach clearly indicate the importance of considering two limiting screening mechanisms, the global dielectric (insulator) screening, embodied in the scaling of the Coulomb interaction by $1/\epsilon_M$, and the short-range metallic screening, represented in the Yukawa potential, for accurate description of the electronic band structure of materials of different nature.

AUTHOR INFORMATION

Corresponding Author

*E-mail: jianghchem@pku.edu.cn.

ORCID

Min-Ye Zhang: 0000-0002-7877-1994

Hong Jiang: 0000-0003-3187-2023

Notes

The authors declare no competing financial interest.

ACKNOWLEDGMENTS

We thank Dr. Joachim Paier for helpful discussion. This work is partly supported by the National Natural Science Foundation of China (Project Numbers 21673005 and 21621061) and the National Key Research and Development Program of China (No. 2016YFB0701100). We acknowledge the High-Performance Computing Platform of Peking University and Tianjin Supercomputer Center for providing computing facility.

REFERENCES

(1) Martin, R. M. *Electronic Structure: Basic Theory and Practical Methods*; Cambridge University Press: Cambridge, U.K., 2004.

(2) Carter, E. A. Challenges in Modeling Materials Properties without Experimental Input. *Science* **2008**, *321*, 800−803.

(3) Jain, A.; Shin, Y.; Persson, K. A. Computational Predictions of Energy Materials Using Density Functional Theory. *Nat. Rev. Mater.* **2016**, *1*, 15004.

(4) Aryasetiawan, F.; Gunnarsson, O. The *GW* Method. *Rep. Prog. Phys.* **1998**, *61*, 237−312.

(5) Perdew, J. P.; Yang, W.; Burke, K.; Yang, Z.; Gross, E. K. U.; Scheffler, M.; Scuseria, G. E.; Henderson, T. M.; Zhang, I. Y.; Ruzsinszky, A.; et al. Understanding Band Gaps of Solids in Generalized Kohn-Sham Theory. *Proc. Natl. Acad. Sci. U. S. A.* **2017**, *114*, 2801−2806.

(6) Rinke, P.; Janotti, A.; Scheffler, M.; Van de Walle, C. G. Defect Formation Energies without the Band-Gap Problem: Combining Density-Functional Theory and the *GW* Approach for the Silicon Self-Interstitial. *Phys. Rev. Lett.* **2009**, *102*, 026402.

(7) Toroker, M. C.; Kanan, D. K.; Alidoust, N.; Isseroff, L. Y.; Liao, P.; Carter, E. A. First Principles Scheme to Evaluate Band Edge Positions in Potential Transition Metal Oxide Photocatalysts and Photoelectrodes. *Phys. Chem. Chem. Phys.* **2011**, *13*, 16644−16654.

(8) Jiang, H.; Shen, Y.-C. Ionization Potentials of Semiconductors from First-Principles. *J. Chem. Phys.* **2013**, *139*, 164114.

(9) Chen, W.; Pasquarello, A. Band-Edge Positions in *GW*: Effects of Starting Point and Self-consistency. *Phys. Rev. B: Condens. Matter Mater. Phys.* **2014**, *90*, 165133.

(10) Grüneis, A.; Kresse, G.; Hinuma, Y.; Oba, F. Ionization Potentials of Solids: The Importance of Vertex Corrections. *Phys. Rev. Lett.* **2014**, *112*, 096401.

(11) Cui, Z.-H.; Jiang, H. Theoretical Investigation of Ta_2O_5, TaON, and Ta_3N_5: Electronic Band Structures and Absolute Band Edges. *J. Phys. Chem. C* **2017**, *121*, 3241−3251.

(12) Wu, F.; Wang, H.; Shen, Y.-C.; Jiang, H. Electronic Properties of Ionic Surfaces: a Systematic Theoretical Investigation of Alkali Halides. *J. Chem. Phys.* **2017**, *146*, 014703.

(13) Perdew, J. P.; Ernzerhof, M.; Burke, K. Rationale for Mixing Exact Exchange with Density Functional Approximations. *J. Chem. Phys.* **1996**, *105*, 9982−9985.

(14) Burke, K.; Ernzerhof, M.; Perdew, J. P. The Adiabatic Connection Method: A Non-Empirical Hybrid. *Chem. Phys. Lett.* **1997**, *265*, 115−120.

(15) Heyd, J.; Scuseria, G. E.; Ernzerhof, M. Hybrid Functionals Based on a Screened Coulomb Potential. *J. Chem. Phys.* **2003**, *118*, 8207.

(16) Heyd, J.; Scuseria, G. E.; Ernzerhof, M. Erratum: "Hybrid Functionals Based on a Screened Coulomb Potential" [J. Chem. Phys.118, 8207 (2003)]. *J. Chem. Phys.* **2006**, *124*, 219906.

(17) Lee, C.; Yang, W.; Parr, R. G. Development of the Colle-Salvetti Correlation-Energy Formula into a Functional of the Electron Density. *Phys. Rev. B: Condens. Matter Mater. Phys.* **1988**, *37*, 785−789.

(18) Becke, A. D. Density-Functional Thermochemistry. III. The Role of Exact Exchange. *J. Chem. Phys.* **1993**, *98*, 5648−5652.

(19) Heyd, J.; Peralta, J. E.; Scuseria, G. E.; Martin, R. L. Energy Band Gaps and Lattice Parameters Evaluated with the Heyd-Scuseria-Ernzerhof Screened Hybrid Functional. *J. Chem. Phys.* **2005**, *123*, 174101.

DOI: 10.1021/acs.jpclett.8b00919
J. Phys. Chem. Lett. 2018, 9, 2338−2345

(20) Paier, J.; Hirschl, R.; Marsman, M.; Kresse, G. The Perdew-Burke-Ernzerhof Exchange-Correlation Functional Applied to the G2−1 Test Set Using a Plane-Wave Basis Set. *J. Chem. Phys.* **2005**, *122*, 234102.
(21) Paier, J.; Marsman, M.; Hummer, K.; Kresse, G.; Gerber, I. C.; Ángyán, J. G. Screened Hybrid Density Functionals Applied to Solids. *J. Chem. Phys.* **2006**, *124*, 154709.
(22) Marsman, M.; Paier, J.; Stroppa, A.; Kresse, G. Hybrid Functionals Applied to Extended Systems. *J. Phys.: Condens. Matter* **2008**, *20*, 064201.
(23) Garza, A. J.; Scuseria, G. E. Predicting Band Gaps with Hybrid Density Functionals. *J. Phys. Chem. Lett.* **2016**, *7*, 4165−4170.
(24) Paier, J. A. *Hartree-Fock Calculations Using Plane Waves*; Ph.D. Thesis, University of Vienna, Vienna, 2007.
(25) Stroppa, A.; Kresse, G. The Shortcomings of Semi-Local and Hybrid Functionals: What We Can Learn from Surface Science Studies. *New J. Phys.* **2008**, *10*, 063020.
(26) Skone, J. H.; Govoni, M.; Galli, G. Self-Consistent Hybrid Functional for Condensed Systems. *Phys. Rev. B: Condens. Matter Mater. Phys.* **2014**, *89*, 195112.
(27) Hedin, L. New Method for Calculating the One-Particle Green's Function with Application to the Electron-Gas Problem. *Phys. Rev.* **1965**, *139*, A796−A823.
(28) Hedin, L.; Lundqvist, B. I. Effects of Electron-Electron and Electron-Phonon Interactions on the One-Electron States of Solids. *Solid State Phys.* **1970**, *23*, 1−181.
(29) Aulbur, W. G.; Jönsson, L.; Wilkins, J. W. Quasiparticle Calculations in Solids. *Solid State Phys.* **2000**, *54*, 1−218.
(30) Rinke, P.; Qteish, A.; Neugebauer, J.; Scheffler, M. Exciting Prospects for Solids: Exact-Exchange Based Functionals Meet Quasiparticle Energy Calculations. *Phys. Status Solidi B* **2008**, *245*, 929−945.
(31) Jiang, H. The *GW* method: Basic Principles, Latest Developments and Its Applications for *d*- and *f*-electron Systems. *Acta Phys.-Chim. Sin* **2010**, *26*, 1017−1033.
(32) Marques, M. A. L.; Vidal, J.; Oliveira, M. J. T.; Reining, L.; Botti, S. Density-Based Mixing Parameter for Hybrid Functionals. *Phys. Rev. B: Condens. Matter Mater. Phys.* **2011**, *83*, 035119.
(33) He, J.; Franchini, C. Assessing the Performance of Self-Consistent Hybrid Functional for Band Gap Calculation in Oxide. *J. Phys.: Condens. Matter* **2017**, *29*, 454004.
(34) Shimazaki, T.; Asai, Y. Band Structure Calculations Based on Screened Fock Exchange Method. *Chem. Phys. Lett.* **2008**, *466*, 91−94.
(35) Skone, J. H.; Govoni, M.; Galli, G. Nonempirical Range-Separated Hybrid Functionals for Solids and Molecules. *Phys. Rev. B: Condens. Matter Mater. Phys.* **2016**, *93*, 235106.
(36) Fritsch, D.; Morgan, B. J.; Walsh, A. Self-Consistent Hybrid Functional Calculations: Implications for Structural, Electronic, and Optical Properties of Oxide Semiconductors. *Nanoscale Res. Lett.* **2017**, *12*, 19.
(37) Henderson, T. M.; Paier, J.; Scuseria, G. E. Accurate Treatment of Solids with the HSE Screened Hybrid. *Phys. Status Solidi B* **2011**, *248*, 767−774.
(38) Gerosa, M.; Bottani, C. E.; Caramella, L.; Onida, G.; di Valentin, C.; Pacchioni, G. Electronic Structure and Phase Stability of Oxide Semiconductors: Performance of Dielectric-Dependent Hybrid Functional DFT, Benchmarked Against *GW* Band Structure Calculations and Experiments. *Phys. Rev. B: Condens. Matter Mater. Phys.* **2015**, *91*, 155201.
(39) Gerosa, M.; Bottani, C. E.; Caramella, L.; Onida, G.; di Valentin, C.; Pacchioni, G. Defect Calculations in Semiconductors through a Dielectric-Dependent Hybrid DFT Functional: The Case of Oxygen Vacancies in Metal Oxides. *J. Chem. Phys.* **2015**, *143*, 134702.
(40) Gaiduk, A. P.; Govoni, M.; Seidel, R.; Skone, J. H.; Winter, B.; Galli, G. Photoelectron Spectra of Aqueous Solutions from First Principles. *J. Am. Chem. Soc.* **2016**, *138*, 6912−6915.
(41) Hinuma, Y.; Kumagai, Y.; Tanaka, I.; Oba, F. Band Alignment of Semiconductors and Insulators Using Dielectric-Dependent Hybrid Functionals: Toward High-Throughput Evaluation. *Phys. Rev. B: Condens. Matter Mater. Phys.* **2017**, *95*, 075302.
(42) Brawand, N. P.; Vörös, M.; Govoni, M.; Galli, G. Generalization of Dielectric-Dependent Hybrid Functionals to Finite Systems. *Phys. Rev. X* **2016**, *6*, 041002.
(43) Bylander, D. M.; Kleinman, L. Good Semiconductor Band Gaps with a Modified Local-Density Approximation. *Phys. Rev. B: Condens. Matter Mater. Phys.* **1990**, *41*, 7868−7871.
(44) Cappellini, G.; del Sole, R.; Reining, L.; Bechstedt, F. Model Dielectric Function for Semiconductors. *Phys. Rev. B: Condens. Matter Mater. Phys.* **1993**, *47*, 9892−9895.
(45) Shimazaki, T.; Asai, Y. First Principles Band Structure Calculations Based on Self-Consistent Screened Hartree-Fock Exchange Potential. *J. Chem. Phys.* **2009**, *130*, 164702.
(46) Shimazaki, T.; Nakajima, T. Dielectric-Dependent Screened Hartree-Fock Exchange Potential and Slater-Formula with Coulomb-Hole Interaction for Energy Band Structure Calculations. *J. Chem. Phys.* **2014**, *141*, 114109.
(47) Seidl, A.; Görling, A.; Vogl, P.; Majewski, J. A.; Levy, M. Generalized Kohn-Sham Schemes and the Band Gap Problem. *Phys. Rev. B: Condens. Matter Mater. Phys.* **1996**, *53*, 3764−3774.
(48) Baer, R.; Livshits, E.; Salzner, U. Tuned Range-Separated Hybrids in Density Functional Theory. *Annu. Rev. Phys. Chem.* **2010**, *61*, 85.
(49) Kresse, G.; Furthmüller, J. Efficient Iterative Schemes for *Ab Initio* Total-Energy Calculations Using a Plane-Wave Basis Set. *Phys. Rev. B: Condens. Matter Mater. Phys.* **1996**, *54*, 11169−11186.
(50) King-Smith, R. D.; Vanderbilt, D. Theory of Polarization of Crystalline Solids. *Phys. Rev. B: Condens. Matter Mater. Phys.* **1993**, *47*, 1651−1654.
(51) Vanderbilt, D.; King-Smith, R. D. Electric Polarization as a Bulk Quantity and Its Relation to Surface Charge. *Phys. Rev. B: Condens. Matter Mater. Phys.* **1993**, *48*, 4442−4455.
(52) Resta, R. Theory of the Electric Polarization in Crystals. *Ferroelectrics* **1992**, *136*, 51−55.
(53) Nunes, R. W.; Gonze, X. Berry-phase Treatment of the Homogeneous Electric Field Perturbation in Insulators. *Phys. Rev. B: Condens. Matter Mater. Phys.* **2001**, *63*, 155107.
(54) Baroni, S.; de Gironcoli, S.; Dal Corso, A.; Giannozzi, P. Phonons and Related Crystal Properties from Density-Functional Perturbation Theory. *Rev. Mod. Phys.* **2001**, *73*, 515−562.
(55) Giannozzi, P.; Baroni, S. In *Handbook of Materials Modeling*; Yip, S., Ed.; Springer: The Netherlands, 2005; pp 195−214.
(56) Gajdoš, M.; Hummer, K.; Kresse, G.; Furthmüller, J.; Bechstedt, F. Linear Optical Properties in the Projector-Augmented Wave Methodology. *Phys. Rev. B: Condens. Matter Mater. Phys.* **2006**, *73*, 045112.
(57) Souza, I.; Iniguez, J.; Vanderbilt, D. First-Principles Approach to Insulators in Finite Electric Fields. *Phys. Rev. Lett.* **2002**, *89*, 117602.
(58) Blöchl, P. E. Projector Augmented-Wave Method. *Phys. Rev. B: Condens. Matter Mater. Phys.* **1994**, *50*, 17953−17979.
(59) Kresse, G.; Joubert, D. From Ultrasoft Pseudopotentials to the Projector Augmented-Wave Method. *Phys. Rev. B: Condens. Matter Mater. Phys.* **1999**, *59*, 1758−1775.
(60) Perdew, J. P.; Burke, K.; Ernzerhof, M. Generalized Gradient Approximation Made Simple. *Phys. Rev. Lett.* **1996**, *77*, 3865−3868.
(61) Goldmann, A.; Chiang, T.; Frank, K.; Koch, E.; Freund, H.; Goldmann, A.; Himpsel, F.; Karlsson, U.; Leckey, R.; Schneider, W. *Electronic Structure of Solids a*; Landolt-Börnstein: Numerical Data and Functional Relationships in Science and Technology, New Series; Springer: Berlin, Heidelberg, 1989.
(62) Shishkin, M.; Kresse, G. Self-consistent *GW* Calculations for Semiconductors and Insulators. *Phys. Rev. B: Condens. Matter Mater. Phys.* **2007**, *75*, 235102.
(63) Jiang, H.; Blaha, P. *GW* with Linearized Augmented Planewaves Extended by High-energy Local Orbitals. *Phys. Rev. B: Condens. Matter Mater. Phys.* **2016**, *93*, 115203.
(64) Madelung, O. *Semiconductors: Data Handbook*, 3rd ed.; Springer-Verlag: New York, 2004.

DOI: 10.1021/acs.jpclett.8b00919
J. Phys. Chem. Lett. 2018, 9, 2338−2345

(65) Chu, J.; Sher, A. *Physics and Properties of Narrow Gap Semiconductors*; Microdevices; Springer: New York, 2010.
(66) Faleev, S. V.; van Schilfgaarde, M.; Kotani, T. All Electron Self-consistent *GW* Approximation: Application to Si, MnO, and NiO. *Phys. Rev. Lett.* **2004**, *93*, 126406.
(67) Shishkin, M.; Marsman, M.; Kresse, G. Accurate Quasiparticle Spectra from Self-Consistent *GW* Calculations with Vertex Corrections. *Phys. Rev. Lett.* **2007**, *99*, 246403.
(68) Vurgaftman, I.; Meyer, J. R.; Ram-Mohan, L. R. Band Parameters for III-V Compound Semiconductors and Their Alloys. *J. Appl. Phys.* **2001**, *89*, 5815−5875.
(69) Davydov, V.; Klochikhin, A.; Seisyan, R.; Emtsev, V.; Ivanov, S.; Bechstedt, F.; Furthmüller, J.; Harima, H.; Mudryi, A.; Aderhold, J.; et al. Absorption and Emission of Hexagonal InN. Evidence of Narrow Fundamental Band Gap. *Phys. Status Solidi B* **2002**, *229*, r1−r3.
(70) Matsuoka, T.; Okamoto, H.; Nakao, M.; Harima, H.; Kurimoto, E. Optical Bandgap Energy of Wurtzite InN. *Appl. Phys. Lett.* **2002**, *81*, 1246−1248.
(71) Wu, J.; Walukiewicz, W.; Yu, K. M.; Ager, J. W.; Haller, E. E.; Lu, H.; Schaff, W. J.; Saito, Y.; Nanishi, Y. Unusual Properties of the Fundamental Band Gap of InN. *Appl. Phys. Lett.* **2002**, *80*, 3967−3969.
(72) Park, J.-W.; Baek, S. H.; Kang, T. D.; Lee, H.; Kang, Y.-S.; Lee, T.-Y.; Suh, D.-S.; Kim, K. J.; Kim, C. K.; Khang, Y. H.; et al. Optical Properties of (GeTe, Sb_2Te_3) Pseudobinary Thin Films Studied with Spectroscopic Ellipsometry. *Appl. Phys. Lett.* **2008**, *93*, 021914.
(73) Park, J.-W.; Eom, S. H.; Lee, H.; da Silva, J. L. F.; Kang, Y.-S.; Lee, T.-Y.; Khang, Y. H. Optical Properties of Pseudobinary GeTe, $Ge_2Sb_2Te_5$, $GeSb_2Te_4$, $GeSb_4Te_7$, and Sb_2Te_3 from Ellipsometry and Density Functional Theory. *Phys. Rev. B: Condens. Matter Mater. Phys.* **2009**, *80*, 115209.
(74) Kim, Y.-S.; Hummer, K.; Kresse, G. Accurate Band Structures and Effective Masses for InP, InAs, and InSb Using Hybrid Functionals. *Phys. Rev. B: Condens. Matter Mater. Phys.* **2009**, *80*, 035203.
(75) Hummer, K.; Grüneis, A.; Kresse, G. Structural and Electronic Properties of Lead Chalcogenides from First Principles. *Phys. Rev. B: Condens. Matter Mater. Phys.* **2007**, *75*, 195211.

DOI: 10.1021/acs.jpclett.8b00919
J. Phys. Chem. Lett. 2018, 9, 2338−2345